N-acetylcysteine alleviates PCB52-induced hepatotoxicity by repressing oxidative stress and inflammatory responses

Wen-Tao Zhou [1], **Li-Bin Wang** [1], **Hao Yu** [2], **Kai-Kai Zhang** [3], **Li-Jian Chen** [3], **Qi Wang** [Corresp., 3], **Xiao-Li Xie** [Corresp. 1]

[1] Department of Toxicology, School of Public Health, Southern Medical University (Guangdong Provincial Key Laboratory of Tropical Disease Research), Guangzhou, China

[2] The 2015 class, 8-Year Program, The First Clinical Medical School, Southern Medical University, Guangzhou, China

[3] Department of Forensic Pathology, School of Forensic Medicine, Southern Medical University, Guangzhou, China

Corresponding Authors: Qi Wang, Xiao-Li Xie
Email address: wangqi_legmed@vip.163.com, xiexiaoli1999@smu.edu.cn

Polychlorinated biphenyls (PCBs), particularly low chlorinated congeners in our environment, can induce human hepatotoxicity. However, the mechanisms by which PCBs cause hepatotoxicity remain elusive. Moreover, there are no effective treatments for this condition. In this study, 40 μM PCB52 was administered to rat (Brl-3A) and human hepatocytes (L-02) for 48 h following the n-acetylcysteine (NAC)/saline pretreatment. A significant decrease in cell viability was observed in PCB52-treated cells relative to the control. Besides, PCB52 significantly increased reactive oxygen species (ROS) levels and malondialdehyde (MDA) contents, suggesting induction of oxidative stress. The expression of *Traf6*, *MyD88*, and *Tnf* in Brl-3A cells and that of *MYD88, TNF, and IL1B* in L-02 cells were significantly upregulated by PCB52. Consistently, overexpression of TLR4, MyD88, Traf6, and NF-κB p65 proteins was observed in PCB52-treated cells, indicating activation of inflammatory responses. Nevertheless, no changes in kelch-like ECH-associated protein 1 (keap1), nuclear factor-erythroid 2-related factor (nrf2), and heme oxygenase-1 proteins were observed in PCB52-treated cells, indicating non-activation of the keap1/nrf2 pathway. Pretreatment with NAC significantly ameliorated PCB52 effects on cell viability, ROS levels, MDA contents and expression of inflammatory elements at both RNA and protein levels. However, no changes in keap1, nrf2 and HO-1 protein levels were detected following NAC pretreatment. Taken together, with non-activated keap1/nrf2 pathway , PCB52-induced oxidative stress and inflammatory responses could be responsible for its hepatotoxicity. These effects were effectively attenuated by NAC pretreatment, which scavenges ROS and dampens inflammatory responses. This study might provide novel strategies for the treatment of the PCBs-associated hepatotoxic effects.

N-Acetylcysteine alleviates PCB52-induced hepatotoxicity by repressing oxidative stress and inflammatory responses

Wen-Tao Zhou[1], Li-Bin Wang[1], Hao Yu[2], Kai-Kai Zhang[3], Li-Jian Chen[3], Qi Wang[3*], Xiao-Li Xie[1*]

1. Department of Toxicology, School of Public Health, Southern Medical University (Guangdong Provincial Key Laboratory of Tropical Disease Research), No. 1838 North Guangzhou Road, 510515 Guangzhou, China
2. The 2015 class, 8-Year Program, The First Clinical Medical School, Southern Medical University, No. 1838 North Guangzhou Road, 510515 Guangzhou, China
3. Department of Forensic Pathology, School of Forensic Medicine, Southern Medical University, No. 1838 North Guangzhou Road, 510515 Guangzhou, China

[*]**Correspondence:**
Corresponding Authors:
Qi Wang, MD, Ph.D., Department of Forensic Pathology, School of Forensic Medicine, Southern Medical University, No. 1838 North Guangzhou Road, 510515 Guangzhou, China
Tel: +86-20-6164-8852,
Fax: +86-20-6164-8359,
E-mail: wangqi_legmed@vip.163.com

Xiao-Li Xie, MD, Ph.D., Department of Toxicology, School of Public Health, Southern Medical University (Guangdong Provincial Key Laboratory of Tropical Disease Research), No. 1838 North Guangzhou Road, 510515 Guangzhou, China
Tel: +86-20-6278-9193,
Fax: +86-20-6164-8324,

E-mail: xiexiaoli1999@126.com, xiexiaoli1999@smu.edu.cn

Abstract

Polychlorinated biphenyls (PCBs), particularly low chlorinated congeners in our environment, can induce human hepatotoxicity. However, the mechanisms by which PCBs cause hepatotoxicity remain elusive. Moreover, there are no effective treatments for this condition. In this study, 40 μM PCB52 was administered to rat (Brl-3A) and human hepatocytes (L-02) for 48 h following the n-acetylcysteine (NAC)/saline pretreatment. A significant decrease in cell viability was observed in PCB52-treated cells relative to the control. Besides, PCB52 significantly increased reactive oxygen species (ROS) levels and malondialdehyde (MDA) contents, suggesting induction of oxidative stress. The expression of *Traf6*, *MyD88*, and *Tnf* in Brl-3A cells and that of *MYD88, TNF, and IL1B* in L-02 cells were significantly upregulated by PCB52. Consistently, overexpression of TLR4, MyD88, Traf6, and NF-κB p65 proteins was observed in PCB52-treated cells, indicating activation of inflammatory responses. Nevertheless, no changes in kelch-like ECH-associated protein 1 (keap1), nuclear factor-erythroid 2-related factor (nrf2), and heme oxygenase-1 proteins were observed in PCB52-treated cells, indicating non-activation of the keap1/nrf2 pathway. Pretreatment with NAC significantly ameliorated PCB52 effects on cell viability, ROS levels, MDA contents and expression of inflammatory elements at both RNA and protein levels. However, no changes in keap1, nrf2 and HO-1 protein levels were detected following NAC pretreatment. Taken together, with non-activated keap1/nrf2 pathway, PCB52-induced oxidative stress and inflammatory responses could be responsible for its hepatotoxicity. These effects were effectively attenuated by NAC pretreatment, which scavenges ROS and

dampens inflammatory responses. This study might provide novel strategies for the treatment of the PCBs-associated hepatotoxic effects.

Keywords: N-acetylcysteine, PCB52, hepatotoxicity, oxidative stress, inflammatory response

1. Introduction

Polychlorinated biphenyls (PCBs) consist of a class of persistent chlorinated pollutants. Theoretically, PCBs are categorized into 209 congeners, including dioxin-like (DL) PCBs and non-DL (NDL) PCBs (Zwierello et al., 2020). Although the production and use of PCBs were banned since the 1970s, their presence in the atmosphere and hydrosphere should be monitored, particularly around the E-waste dump sites (Prithiviraj and Chakraborty, 2020). Due to their characteristic high persistence and bioaccumulation, PCBs are harmful to both animals and humans, even at low levels (Elnar et al., 2015). The toxic effects of DL-PCBs are primarily implemented via activation of the aryl hydrocarbon receptor (AhR) pathway (Du et al., 2019; Fabelova et al., 2019). In the air, PCBs mainly exist as low-chlorinated congeners (Halsall et al., 1995). Notably, NDL low-chlorinated PCBs induce higher oxidative stress levels (Pessah et al., 2019) and are more toxic than DL PCBs (Hansen, 1998). However, the mechanisms of toxicity induction by NDL PCBs are obscure. The presence of PCB52, known as an indicator PCB, has been demonstrated in food, human blood and milk (Brunelli et al., 2012). Exposure to PCB52 causes alterations in motor activity (Boix et al., 2011), impairment of neurodevelopment (Pessah et al., 2019), and an impaired sense of hearing (Fabelova et al., 2019). *In vitro* exposure to PCB52

induces excessive generation of reactive oxygen species (ROS) in hepatocytes (Wang et al., 2018). Subsequently, the high ROS levels increase the release of inflammatory mediators (Song et al., 2020), through their effect on toll-like receptors (TLRs)/myeloid differentiation primary response 88 (MyD88) pathway (Steckling et al., 2020). These effects can also be executed via the Kelch-like ECH-associated protein 1(Keap1)/nuclear factor-erythroid 2-related factor (Nrf2)/heme oxygenase-1 (HO-1) pathway, which has both antioxidant and anti-inflammatory effects (Nguyen et al., 2009; Song et al., 2020; Yamamoto et al., 2018). Moreover, MyD88-dependent TLR4 mediates accumulation of p62 (also known as SQSTM1), which plays an important role in degradation of autophagosomes (Fujita et al. 2011). Aberrant accumulation of p62 results in entrapment of Keap1 and activation of Nrf2 (Komatsu et al. 2010).

Overgeneration of ROS is contributed to PCBs-induced hepatotoxicity (Wang et al., 2018). ROS accumulation can result in releases of inflammatory mediators, which take an important role in hepatotoxicity (Khan et al. 2019). We hypothesized that PCBs-induced excessive generation of ROS and ROS-initiated releases of inflammatory mediators might be responsible for PCBs-induced hepatotoxicity. In the present study, rat (Brl-3A) and human hepatocytes (L-02) were pre-treated with N-acetylcysteine (NAC), a scavenger of ROS, and then exposed to PCB52. The effect of NAC on the rats and human hepatocytes was assessed by determining cell viability, ROS levels, malondialdehyde (MDA) contents, inflammatory, and the activity of the Keap1/Nrf2 pathway. Our findings could provide a novel strategy for the prevention and treatment of PCB52-induced hepatotoxicity.

2. Materials and Methods

2.1 Special chemicals and cell lines

PCB52 (2,2',5,5'-tetrachlorodiphenyl, purity of 99.4%) was procured from J&K Scientific Company (Beijing, China) and dissolved in dimethylsulfoxide (DMSO) to prepare a 100 mM stock solution. N-acetylcysteine (NAC), and 2',7'-Dichlorodihydrofluorescein diacetate (DCFH-DA) were purchased from Sigma Chemical Co (USA). A 600 mmol/L stock solution of NAC was prepared by dissolving solid NAC in saline. Normal human hepatocytes, cell line L-02 (HL-7702) and normal rat hepatocytes, cell line Brl-3A were obtained from the Typical Culture Preservation Commission Cell Bank, Chinese Academy of Sciences, Shanghai, China.

2.2 Cell culture and treatments

Human L-02 cells were cultured in Roswell Park Memorial Institute (RPMI) 1640 medium (Gibco) supplemented with 15% fetal bovine serum (FBS) and 100 U/ml penicillin‐streptomycin. Rat Brl-3A cells were cultured in Dulbecco minimum essential medium (DMEM, Gibco) supplemented with 3% FBS and 100 U/ml penicillin‐streptomycin. Cells were cultured at 37°C in a thermostatic incubator (Thermo Fisher Scientific Inc., USA) infused with carbon dioxide concentration 5%, and 95% saturated atmospheric humidity.

Cells (passage 10) were randomly divided into four groups, including the control, PCB52, NAC, and NAC + PCB52 groups. Following the results of our preliminary experiments (Supplementary Fig. 1), Brl-3A cells were pretreated with 3 mM NAC for 12 h, while human L-02 cells were pretreated with 1 mM NAC for 6 h (Gu et al., 2018). The cells were then exposed to

40 μM PCB52 for 48 h and used for subsequent experiments. PCB52 exerted dose- and time-dependent effects (Wang et al., 2018). The concentration of PCB52 and the exposure duration were chosen based on our previous study (Wang et al., 2018) and the changes of cell viabilities in our preliminary experiments.

2.3 Determination of cell viability

Cell viability was determined using the cell counting kit-8 (CCK-8, Dojindo, Japan) according to the manufacturer's instructions. In brief, cells were first seeded on a 96-well plate. The culture medium was replaced with medium containing PCB52 concentrations of 0, 10, 20, 40 and 80 μmol/L and incubated for 48 h. Then, the PCB media was replaced with a basal medium containing 10 μl of CCK-8 solution and incubated for 3 h at 37°C. Finally, the absorbance was assessed at 450 nm using a microplate reader (Bio-rad model 680, BIO-RAD, USA).

2.4 Monitoring ROS levels

The cells, both L-02 (5×10^5 cells/ml) and Brl-3A (2×10^5 cells/ml) were seeded in 25 cm^2 canted-neck tissue culture flasks (Corning, NY, 14831, USA) and then treated as previously mentioned. Cells were washed twice with PBS, incubated with 10 μmol/L DCFH-DA for 30 min at 37°C, digested by 0.25% trypsin and washed three times with ice-cold PBS.DCFH-DA fluorescence was analyzed by flow cytometry (BD LSRFortessa™, BD, CA, USA).

2.5 Examinations of MDA contents

Briefly, the MDA levels were evaluated using an MDA assay kit (Nanjing Jiancheng Bioengineering Institute, Nanjing, China), according to the operation manual. Optical densities of the supernatants were read at 532 nm using a microplate reader (Bio-rad model 680, BIO-RAD, USA) and the protein concentrations of cells were determined using the Pierce™ BCA Protein Assay Kit (Thermo Fisher Scientific Inc., USA). The MDA contents are presented as nmol per mg protein in the bar graph.

2.6 Real-time Quantitative PCR (RT-qPCR)

Total RNA was extracted using TRIzol® Reagent (Thermo Fisher Scientific, USA), and the RNA quality and quantity were measured using a NanoDrop2000 Spectrophotometer (Thermo Fisher Scientific, MA, USA). Complementary DNA (cDNA) was synthesized from the total RNA using the Prime Script RT Reagent Kit (RR036A, Takara Biotechnology Co., LTD). Primers for tumor necrosis factor (TNF) receptor-associated factor 6 (*Traf6*), myeloid differentiation factor88 (*MyD88*), *TNF*, interleukin (*IL*)*1B*, *Keap1*, *Nfe2l2*/*Nrf2*, heme oxygenase (*Hmox*/*HO*)-*1*, NAD(P)H quinone oxidoreductase 1 (*NQO1*), *Sqstm1*/*P62*, and *β-actin* were designed using the Get Prime software (https://gecftools.epfl.ch/getprime). Real-time Quantitative PCR (RT-qPCR) was conducted using TB Green™ Premix Ex Taq™ GC (RR820A, Takara) on a Light Cycler® 96 System (Roche Life Science). Relative quantification of gene expression was performed based on the comparative CT ($2^{-\triangle\triangle}$Ct) method. The mRNA expression levels of target genes were normalized to that of the *β-actin* internal standard. Data were presented as fold changes over the controls, which were shown as 1. The sequences of primers used for RT-qPCR are shown in

Supplementary Table 1.

2.7 Western blot analysis

Total protein was extracted by lysis using a RIPA buffer (containing 1 mmol/L PMSF), 30 min incubation in ice, and total proteins were collected. Protein concentrations were determined using a Pierce™ BCA Protein Assay Kit (Thermo Fisher Scientific, USA). Proteins (20 μg per sample) were separated by SDS-polyacrylamide gel electrophoresis (PAGE) and transferred to polyvinylidene difluoride (PVDF) membranes (BIO-RAD). The membranes were then blocked with 5% milk-Tris-buffered-Tween solution for 2 h at room temperature, incubated with primary antibodies at 4°C overnight, followed by incubation in the appropriate secondary antibodies. Finally, blots were incubated in enhanced chemiluminescent (ECL) detection reagent (BIO-RAD Laboratories, Inc., California, USA) for 3 min. Densitometric analysis was performed using the Tanon Gel Image System (version 4.2). Band intensities were normalized using GAPDH as an internal control. Data on relative integrated optical density values of bands are displayed in the form of bar charts, with the control presented as 1. This study used primary antibodies against toll-like receptor 4 (TLR4, dilution 1:5000, sc293072, Santa Cruz Biotechnology), Traf6 (dilution 1:3000, sc8409, Santa Cruz Biotechnology), MyD88 (dilution 1:3000, sc-74532, Santa Cruz), Nrf2 (dilution 1:2000, sc-13032, Santa Cruz), keap1 (dilution 1:3000, sc-15246, Santa Cruz), HO-1 (dilution 1:2000, sc-390991, Santa Cruz), NF-κB p65 (dilution 1:2000, sc-8008, Santa Cruz) and GAPDH (dilution 1:5000, sc-32233, Santa Cruz).

176 **2.8 Statistical analysis**

177 Numeric data are presented as mean ± standard error (SE) of at least three independent
178 replicates. Statistical analysis was conducted using the SPSS statistical software (version 16.0,
179 IBM, USA). Differences in mean values between the control and PCB52-treated cells were
180 evaluated by the Independent-Samples T-test, while differences between the control, PCB52,
181 NAC, and NAC + PCB52 groups were analyzed by One-Way analysis of variance (ANOVA). A
182 p-value < 0.05 was considered statistically significant.

183

184 **3. Results**

185 **3.1 NAC pretreatment alleviates PCB52-induced hepatotoxicity**

186 Compared to the control group, 48 h exposure of Brl-3A and L-02 cells to PCB52 reduced cell
187 viabilities in a dose-dependent manner (Supplemental Fig. 1). The most significant reduction was
188 obtained at PCB52 concentrations of 40 and 80 μM. Consistent with our previous study (Wang et
189 al., 2018), a PCB52 concentration of 40 μM was found as the most suitable for further studies.

190 Compared with the control, no significant changes in Brl-3A cell viabilities were observed
191 following 12 h NAC pre-treatment at concentrations 3, 5, and 10 mM. Pretreatment with NAC at
192 concentrations 3 and 5 mM significantly ameliorated PCB52-induced cytotoxicity in Brl-3A cells
193 (Supplemental Fig. 2). Accordingly, 3 mM NAC was chosen to perform subsequent analyses.
194 Similar to the findings of our preliminary experiment, NAC pretreatment significantly repressed
195 PCB52-induced hepatotoxicity in Brl-3A cells (Fig. 1A). In L-02 cells also, cell viability
196 significantly increased in the NAC + PCB52 group compared with the PCB52 group (Fig. 1B),

while no change in cell viability was observed in the NAC group compared with the control (Fig. 1).

3.2 NAC pretreatment mitigated PCB52-induced ROS accumulation and MDA content

The levels of ROS in PCB52-treated cells were significantly higher than in control groups (Fig. 2 A-B). Compared with the PCB52 group, NAC pretreatment significantly reduced ROS levels in both Brl-3A (Fig. 2A) and L-02 cells (Fig. 2B). However, no significant changes in ROS levels were observed between the NAC group and the control group.

Moreover, MDA contents in PCB52-treated Brl-3A and L-02 cells were considerably higher than in control groups (Fig. 2 C-D). Consistently, NAC pretreatment significantly reduced MDA content compared to the PCB52 group. However, no significant differences in MDA content were observed between the NAC group and the control group.

3.3 NAC pretreatment reduces PCB52-induced inflammatory response

In Brl 3A cells, compared to the control group, the expression of *Traf6*, *MyD88*, and *Tnf* were significantly increased in PCB52 group (Fig. 3A), indicating activation of inflammatory pathways. Also, the expression of *Hmox1*, *Nqo1*, and *Sqstm1* was significantly upregulated by exposure to PCB52, while no significant changes were detected in the expression levels of *Keap1* and *Nfe2l2* (Fig. 3B). NAC pretreatment significantly reduced expression of *Traf6*, *MyD88*, and *Tnf* as compared to the PCB52 group (Fig. 3A), while no significant changes in the expression of *Keap1*, *Nfe2l2*, *Hmox1*, *Nqo1*, and *Sqstm1* were observed (Fig. 3B). Besides, no significant changes in

gene expression were observed between the NAC group and the control group. Downregulated expression of *Hmox1* in the NAC + PCB52 group could suggest a reduction of a compensatory response to an oxidative and inflammatory reaction. However, no significant changes in the expression of *Keap1*, *Nfe2l2*, *Nqo1*, and *Sqstm1* were observed.

In L-02 cells, compared with the control, the expression of *MYD88, TNF, and IL1B* were significantly upregulated in PCB52 group (Fig. 3C), while no significant changes were detected in the expression levels of *TRAF6*, *KEAP1*, *NFE2L2*, *HMOX1*, and *NQO1* (Fig. 3D). Expression of *MYD88*, *TNF*, and *IL1B* was significantly decreased in the NAC + PCB52 group compared with the PCB52 group (Fig. 3C). However, no significant changes in the expression of *TRAF6*, *KEAP1*, *NFE2L2*, *HMOX1*, and *NQO1* were observed between the two groups. Also, no significant difference was found in the NAC group compared with the control group.

Consistent with the RNA levels, western blot analysis showed that the protein expression of TLR4, MyD88, Traf6, and NF-κB p65 was significantly increased in PCB52-treated Brl-3A cells, as compared with the control (Fig. 4 A-E). However, no significant changes were observed in the protein expression of keap1, Nrf2, and HO-1 (Fig. 4 A and F-H). Furthermore, overexpression of TLR4, MyD88, Traf6, and NF-κB p65 proteins was also observed in PCB52-treated L-02 cells (Fig. 4 I-M). Meanwhile, no significant changes in the expression of keap1, Nrf2, and HO-1 proteins were found (Fig. 4 I and N-P), which concurs with the observations made in Brl-3A cells. Furthermore, expression of TLR4, MyD88, Traf6, and NF-κB p65 proteins was significantly repressed in the NAC + PCB52 group compared with the PCB52 group in both Brl-3A (Fig. 4 A-E) and L-02 cells (Fig. 4 I-M), suggesting reduced inflammation following NAC pretreatment.

239 However, no significant changes in keap1, Nrf2, and HO-1 proteins were observed.

240

241 **4. Discussion**

242 Polychlorinated biphenyls (PCBs), particularly low chlorinated PCBs, can currently be
243 detected in our environment and animal tissues (Wu et al., 2020). However, the underlying
244 mechanisms of PCB-induced hepatotoxicity, as well as effective treatment for the condition, are
245 indistinct. The findings of the present study showed that PCB52, an indicator of PCBs, induces
246 apparent hepatotoxicity in both Brl-3A and L-02 cells, which is consistent with our previous study
247 results (Wang et al., 2018). Moreover, significantly increased ROS levels and MDA contents were
248 detected in cells treated with PCB52. Overgeneration of ROS and dysfunction of the antioxidant
249 system results in an imbalance of redox homeostasis and elevated oxidative stress levels (Chang
250 et al., 2019). In this study, elevated ROS levels indicate induction of oxidative stress, which was
251 confirmed by the augmented MDA, a product of polyunsaturated fatty acid (PUFA) peroxidation,
252 which is a component of biological membranes (Tsikas, 2017). Furthermore, induction of
253 oxidative stress may result in cell death (Pirozzi et al., 2020).

254 Notably, the overproduction of ROS promotes the release of inflammatory mediators,
255 including TNF-α and IL-1β, via activation of the TLR4/MyD88 pathway (Gong et al., 2019; Shah
256 et al., 2019; Steckling et al., 2020). The transmembrane protein TLR4 is a vital member of the toll-
257 like receptor family, and its interaction with the adaptors MyD88 and TRAF6 are essential for
258 activation of downstream elements and induction of inflammatory response (Dasu and Jialal,
259 2013). In the present study, PCB52 significantly upregulated the expression of *Traf6*, *MyD88*, and

260 *Tnf* in Brl-3A cells, while *MYD88*, *TNF*, and *IL1B* levels were significantly increased in PCB52-
261 treated L-02 cells compared with the control. Consistent with the RNA results, increased
262 expression of TLR4, MyD88, Traf6, and NF-κB p65 proteins were observed in PCB52-treated
263 Brl-3A and L-02 cells, indicating activation of inflammatory responses.

264 We also found that PCB52 significantly induced the expression of *Hmox1*, *Nqo1*, and *Sqstm1*
265 in Brl-3A cells, while no changes in the gene expression patterns of *Keap1* and *Nfe2l2* were
266 observed. In PCB52-treated L-02 cells, no changes in the expression of *KEAP1*, *NFE2L2*,
267 *HMOX1*, and *NQO1* were observed relative to the control. Moreover, no significant changes in the
268 protein expression of keap1, Nrf2, and HO-1 were detected in PCB52-treated Brl-3A and L-02
269 cells, suggesting the non-activation of the keap1/Nrf2 pathway, regardless of overproduction of
270 ROS. However, the exact cause of this non-activation needs further investigation. The Keap1/Nrf2
271 pathway can activate protein HO-1 and is considered to exert anti-oxidant and anti-inflammation
272 effects (Maamoun et al., 2019). As an important factor of anti-oxidative stress and anti-
273 inflammatory (Gozzelino et al. 2010; Willis et al. 1996), *Hmox-1* gene expression can be mediated
274 by redox-dependent transcription factors (the keap1/Nrf2 system, the transcription repressor
275 Bach1, NF-κB, activating protein-1) and signaling cascades (p38 MAPK, the phosphatidylinositol-
276 3 kinase/AKT pathway, IL-10 and the Jak-STAT pathway, the TLR-4 pathway) (Naito et al. 2014;
277 Paine et al. 2010). In the present study, increased gene and protein expression of Traf6 and Myd88
278 as well as overexpression of protein TLR4 might contribute to the up-regulation of gene *Hmox-1*
279 in PCB52-treated Brl-3A cells, although no change of its protein was observed. The result was
280 consistent with previous studies (Andreas et al. 2018; Doberer et al. 2010). No change of protein

281 expression of HO-1 might be attributed to the mediators of multi signaling cascades and redox-
282 dependent transcription factors as well as the usage and degradation of HO-1 protein (Andreas et
283 al. 2018; Doberer et al. 2010). In this case, the exact mechanisms of the non-parallel expression of
284 the *Hmox-1* mRNA and its protein need further experiments to clarify. Besides the overproduction
285 of ROS and MDA; therefore, the mute keap1/Nrf2 pathway might exacerbate oxidative stress and
286 cell death.

287 Nevertheless, pretreatment with NAC, which is a known ROS scavenger, significantly
288 ameliorated PCB52-induced reduction of cell viability, suggesting that elimination of ROS could
289 alleviate PCB52-induced hepatotoxicity. In the NAC + PCB52 group, the ROS level and MDA
290 content were significantly reduced relative to the PCB52 group, indicating repression of oxidative
291 stress. Furthermore, expression of *Traf6*, *MyD88*, and *Tnf* in Brl-3A cells and that of *MYD88*, *TNF*
292 and *IL1B* in L-02 cells as well as TLR4, MyD88, Traf6, and NF-κB p65 proteins in the two cell
293 types were significantly decreased following NAC pretreatment. This observation suggests a
294 dampened inflammatory response due to ROS elimination, which concurs with the findings of our
295 previous study (Li et al., 2020). In Brl-3A cells also, *Hmox1* was downregulated by pretreatment
296 with NAC, which was consistent with the repressions of the ROS level and MDA content. In
297 addition, compared with the control, gene expression of *Traf6*, *Hmox1*, and *Nqo1* were significant
298 upregulated in PCB52-treated Brl-3A cells but not in L-02 cells, suggesting different sensitivities
299 of cells from different species to PCB52 exposure.

300 In our previous study (Wang et al., 2018), the activation of autophagy resulted in the increase
301 of autophagosomes. The deficit cleavage of autophagosomes induced the blocked autophagic flux,

which contributed to PCB52-induced hepatotoxicity. Therefore, the usage of 3-methlyadenine (3-MA), an inhibitor of autophagy, alleviated the activated autophagy, the blocked autophagic flux and PCB52-induced hepatotoxicity. Because of the attenuated initiation of autophagy, the positive feedback loop of autophagy and ROS was repressed and ROS levels were significantly decreased by the treatment of 3-MA. However, whether the scavenger-mediated decrease of ROS levels could weaken PCB52-induced hepatotoxicity and the exact mechanisms are unclear. In the present study, the usage of NAC significantly decreased ROS levels and MDA contents, suppressed overexpression of TLR4 pathway, and attenuated PCB52-induced hepatotoxicity, although no change of proteins of keap1/Nrf2 pathway was observed. These results suggested that PCB52 induced hepatotoxicity by initiation of oxidative stress and activation of ROS-mediated inflammatory pathway.

In summary, PCB52-induced oxidative stress, inflammatory responses, and inactive keap1/Nrf2 pathway could be responsible for its hepatotoxicity *in vitro* (Fig. 5). Notably, all these effects were effectively alleviated by NAC pretreatment, which acts via the elimination of ROS and repression of inflammatory responses (Fig. 5). The findings of this study could provide novel strategies for the treatment and prevention of the hepatotoxic effects associated with exposure to PCBs.

Conflict of Interest

The authors declare that the research was conducted in the absence of any commercial or

322 financial relationships that could be construed as a potential conflict of interest.

323

324 **Author Contributions**

325 Zhou Wen-Tao: Investigation, Software, Data Curation, Writing - Original Draft; Wang Li-
326 Bin: Investigation, Software, Formal analysis; Yu Hao: Validation, Software; Zhang Kai-Kai:
327 Formal analysis, Visualization; Chen Li-Jian: Validation; Wang Qi:Conceptualization, Project
328 administration, Funding acquisition;Xie Xiao-Li: Methodology, Supervision, Funding acquisition,
329 Writing - Review & Editing.

330

331 **Funding**

332 The study was supported by the National Natural Science Foundation of China (Grant No.
333 81601641 and 81871526), the Guangdong Natural Science Foundation (Grant No.
334 2014A030310504 and 2020A1515010370), the Scientific Research Foundation for the Returned
335 Overseas Chinese Scholars, the National Education Ministry (Grant No. 2015-311).

336

337 **References**

338 Andreas, M., Oeser, C., Kainz, F. M., Shabanian, S., Aref, T., Bilban, M., Messner, B., Heidtmann,
339 J., Laufer, G., Kocher, A., Wolzt, M., 2018. Intravenous Heme Arginate Induces HO-1 (Heme
340 Oxygenase-1) in the Human Heart. Arterioscler Thromb Vasc Biol 38(11), 2755-2762.
341 10.1161/ATVBAHA.118.311832.
342 Boix, J., Cauli, O., Leslie, H., Felipo, V., 2011. Differential long-term effects of developmental
343 exposure to polychlorinated biphenyls 52, 138 or 180 on motor activity and

neurotransmission. Gender dependence and mechanisms involved. NeurochemInt 58, 69-77. 10.1016/j.neuint.2010.10.014.

Brunelli, L., Llansola, M., Felipo, V., Campagna, R., Airoldi, L., De Paola, M., Fanelli, R., Mariani, A., Mazzoletti, M., Pastorelli, R., 2012. Insight into the neuroproteomics effects of the food-contaminant non-dioxin like polychlorinated biphenyls. J Proteomics 75, 2417-2430. 10.1016/j.jprot.2012.02.023.

Chang, X., Wang, X., Feng, J., Su, X., Liang, J., Li, H., Zhang, J., 2019. Impact of chronic exposure to trichlorfon on intestinal barrier, oxidative stress, inflammatory response and intestinal microbiome in common carp (Cyprinuscarpio L.). Environ Pollut 259, 113846. 10.1016/j.envpol.2019.113846.

Dasu, M.R., Jialal, I., 2013. Amelioration in wound healing in diabetic toll-like receptor-4 knockout mice. J Diabetes Complications 27, 417-421. 10.1016/j.jdiacomp.2013.05.002.

Doberer, D., Haschemi, A., Andreas, M., Zapf, T. C., Clive, B., Jeitler, M., Heinzl, H., Wagner, O., Wolzt, M., Bilban, M., 2010. Haem arginate infusion stimulates haem oxygenase-1 expression in healthy subjects. Br J Pharmacol 161(8), 1751-1762. 10.1111/j.1476-5381.2010.00990.x.

Du, F., Zhao, T., Ji, H.C., Luo, Y.B., Wang, F., Mao, G.H., Feng, W.W., Chen, Y., Wu, X.Y., Yang, L.Q., 2019. Dioxin-like (DL-) polychlorinated biphenyls induced immunotoxicity through apoptosis in mice splenocytes via the AhR mediated mitochondria dependent signaling pathways. Food ChemToxicol 134, 110803. 10.1016/j.fct.2019.110803.

Elnar, A.A., Desor, F., Marin, F., Soulimani, R., Nemos, C., 2015. Lactational exposure to low levels of the six indicator non-dioxin-like polychlorinated biphenyls induces DNA damage and repression of neuronal activity, in juvenile male mice. Toxicology 328, 57-65. 10.1016/j.tox.2014.12.011.

Fabelova, L., Loffredo, C.A., Klanova, J., Hilscherova, K., Horvat, M., Tihanyi, J., Richterova, D., PalkovicovaMurinova, L., Wimmerova, S., Sisto, R., Moleti, A., Trnovec, T., 2019. Environmental ototoxicants, a potential new class of chemical stressors. Environ Res 171, 378-394. 10.1016/j.envres.2019.01.042.

Fujita, K., Maeda, D., Xiao, Q., Srinivasula, S. M., 2011. Nrf2-mediated induction of p62 controls Toll-like receptor-4-driven aggresome-like induced structure formation and autophagic degradation. Proc Natl Acad Sci U S A 108(4), 1427-1432. 10.1073/pnas.1014156108.

Gong, T., Jiang, W., Gao, Z., Chen, Y., Gao, S., 2019. Dibromoacetic Acid Induced Hepatotoxicity in Mice through Oxidative Stress and Toll-Like Receptor 4 Signaling Pathway Activation. Oxid Med Cell Longev 2019, 5637235. 10.1155/2019/5637235.

Gozzelino, R., Jeney, V., Soares, M. P., 2010. Mechanisms of cell protection by heme oxygenase-1. Annu Rev Pharmacol Toxicol 50, 323-354. 10.1146/annurev.pharmtox.010909.105600.

Gu, L.L., Shen, Z.L., Li, Y.L., Bao, Y.Q., Lu, H., 2018. Oxymatrine Causes Hepatotoxicity by Promoting the Phosphorylation of JNK and Induction of Endoplasmic Reticulum Stress Mediated by ROS in LO2 Cells. Mol Cells 41, 401-412. 10.14348/molcells.2018.2180.

Halsall, C.J., Lee, R.G., Coleman, P.J., Burnett, V., Harding-Jones, P., Jones, K.C., 1995. PCBs in U.K. Urban Air. Environ SciTechnol 29, 2368-2376. 10.1021/es00009a032.

Hansen, L.G., 1998. Stepping backward to improve assessment of PCB congener toxicities. Environ Health Perspect 106 Suppl 1, 171-189. 10.1289/ehp.98106s1171.

Khan, H., Ullah, H., Nabavi, S. M., 2019. Mechanistic insights of hepatoprotective effects of curcumin: Therapeutic updates and future prospects. Food Chem Toxicol 124, 182-191. 10.1016/j.fct.2018.12.002.

Komatsu, M., Kurokawa, H., Waguri, S., Taguchi, K., Kobayashi, A., Ichimura, Y., Sou, Y. S., Ueno, I., Sakamoto, A., Tong, K. I., Kim, M., Nishito, Y., Iemura, S., Natsume, T., Ueno, T., Kominami, E., Motohashi, H., Tanaka, K., Yamamoto, M., 2010. The selective autophagy substrate p62 activates the stress responsive transcription factor Nrf2 through inactivation of Keap1. Nat Cell Biol 12(3), 213-223. 10.1038/ncb2021.

Li, H., Bai, Z., Li, C., Sheng, C., Zhao, X., 2020. EV71 infection induces cell apoptosis through ROS generation and SIRT1 activation. J Cell Biochem. 10.1002/jcb.29628.

Maamoun, H., Benameur, T., Pintus, G., Munusamy, S., Agouni, A., 2019. Crosstalk Between Oxidative Stress and Endoplasmic Reticulum (ER) Stress in Endothelial Dysfunction and Aberrant Angiogenesis Associated With Diabetes: A Focus on the Protective Roles of HemeOxygenase (HO)-1. Front Physiol 10, 70. 10.3389/fphys.2019.00070.

Naito, Y., Takagi, T., Higashimura, Y., 2014. Heme oxygenase-1 and anti-inflammatory M2 macrophages. Arch Biochem Biophys 564, 83-88. 10.1016/j.abb.2014.09.005.

Nguyen, T., Nioi, P., Pickett, C.B., 2009. The Nrf2-antioxidant response element signaling pathway and its activation by oxidative stress. J BiolChem 284, 13291-13295. 10.1074/jbc.R900010200.

Paine, A., Eiz-Vesper, B., Blasczyk, R., Immenschuh, S., 2010. Signaling to heme oxygenase-1 and its anti-inflammatory therapeutic potential. Biochem Pharmacol 80(12), 1895-1903. 10.1016/j.bcp.2010.07.014.

Pessah, I.N., Lein, P.J., Seegal, R.F., Sagiv, S.K., 2019. Neurotoxicity of polychlorinated biphenyls and related organohalogens. ActaNeuropathol 138, 363-387. 10.1007/s00401-019-01978-1.

Pirozzi, C., Lama, A., Annunziata, C., Cavaliere, G., De Caro, C., Citraro, R., Russo, E., Tallarico, M., Iannone, M., Ferrante, M.C., Mollica, M.P., MattaceRaso, G., De Sarro, G., Calignano, A., Meli, R., 2020. Butyrate prevents valproate-induced liver injury: In vitro and in vivo evidence. FASEB J 34, 676-690. 10.1096/fj.201900927RR.

Prithiviraj, B., Chakraborty, P., 2020. Atmospheric polychlorinated biphenyls from an urban site near informal electronic waste recycling area and a suburban site of Chennai city, India. Sci Total Environ 710, 135526. 10.1016/j.scitotenv.2019.135526.

Shah, H.K., Sharma, T., Banerjee, B.D., 2019. Organochlorine pesticides induce inflammation, ROS production, and DNA damage in human epithelial ovary cells: An in vitro study. Chemosphere 246, 125691. 10.1016/j.chemosphere.2019.125691.

Song, C., Heping, H., Shen, Y., Jin, S., Li, D., Zhang, A., Ren, X., Wang, K., Zhang, L., Wang, J., Shi, D., 2020. AMPK/p38/Nrf2 activation as a protective feedback to restrain oxidative stress and inflammation in microglia stimulated with sodium fluoride. Chemosphere 244, 125495. 10.1016/j.chemosphere.2019.125495.

426 Steckling, F.M., Lima, F.D., Farinha, J.B., Rosa, P.C., Royes, L.F.F., Cuevas, M.J., Bresciani, G.,
427 Soares, F.A., Gonzalez-Gallego, J., Barcelos, R.P., 2020. Diclofenac attenuates inflammation
428 through TLR4 pathway and improves exercise performance after exhaustive swimming.
429 Scand J Med Sci Sports 30, 264-271. 10.1111/sms.13579.
430 Tsikas, D., 2017. Assessment of lipid peroxidation by measuring malondialdehyde (MDA) and
431 relatives in biological samples: Analytical and biological challenges. Anal Biochem 524, 13-
432 30. 10.1016/j.ab.2016.10.021.
433 Wang, Q., Wei, L.W., Zhou, W.T., Wang, Z.T., Xie, X.L., 2018. PCB28 and PCB52 induce
434 hepatotoxicity by impairing the autophagic flux and stimulating cell apoptosis in vitro.
435 ToxicolLett 289, 28-41. 10.1016/j.toxlet.2018.03.002.
436 Willis, D., Moore, A. R., Frederick, R., Willoughby, D. A., 1996. Heme oxygenase: a novel target
437 for the modulation of the inflammatory response. Nat Med 2(1), 87-90. 10.1038/nm0196-87.
438 Wu, J.P., Peng, Y., Zhi, H., Wu, S.K., Chen, X.Y., Zeng, Y.H., Luo, X.J., Mai, B.X., 2020.
439 Contaminant-related oxidative distress in common kingfisher (Alcedoatthis) breeding at an
440 e-waste site in South China. Environ Res 182, 109079. 10.1016/j.envres.2019.109079.
441 Yamamoto, M., Kensler, T.W., Motohashi, H., 2018. The KEAP1-NRF2 System: a Thiol-Based
442 Sensor-Effector Apparatus for Maintaining Redox Homeostasis. Physiol Rev 98, 1169-1203.
443 10.1152/physrev.00023.2017.
444 Zwierello, W., Maruszewska, A., Skorka-Majewicz, M., Goschorska, M., Baranowska-Bosiacka,
445 I., Dec, K., Styburski, D., Nowakowska, A., Gutowska, I., 2020. The influence of polyphenols
446 on metabolic disorders caused by compounds released from plastics - Review. Chemosphere
447 240, 124901. 10.1016/j.chemosphere.2019.124901.

449 **Figure legends**

450

451 Figure 1. Detection of cell viabilities by CCK-8 assay. N-Acetylcysteine (NAC) pretreatment
452 significantly attenuated PCB52-induced cytotoxicity in both Brl-3A (A) and L-02 cells (B), while
453 no significant changes in cell viability were observed in the NAC group compared with the control.
454 $^{**}p < 0.01$, compared with the control; $\#p < 0.05$, $\#\#p < 0.01$, compared with the PCB52 group.

455

456 Figure 2. Examination of intracellular ROS levels and MDA contents. A-B, PCB52-induced
457 increase in ROS levels was significantly inhibited by NAC pretreatment in both Brl-3A (A) and
458 L-02 cells (B), while no significant changes in ROS levels were detected in the NAC group
459 compared with the control. C-D, The increase in MDA contents following the administration of
460 PCB52 was significantly repressed by pretreatment with NAC in both Brl-3A (C) and L-02 cells
461 (D). No significant changes in MDA contents were observed in the NAC group compared with the
462 control. $^{**}p < 0.01$, compared with the control; $\#p < 0.05$, $\#\#p < 0.01$, compared to the PCB52
463 group.

464

465 Figure 3. RT-qPCR analysis for assessment of *Traf6*, *MyD88*, *Tnf*, *IL1B*, *Keap1*, *Nfe2l2*, *Hmox1*,
466 *Nqo1*, and *Sqstm1* gene expression. A-B, In Brl-3A cells, the upregulation of *Traf6*, *MyD88*, *Tnf*,
467 and *Hmox1* was significantly reduced in the NAC + PCB52 group relative to the PCB52 group,
468 while no changes in the expression of *Keap1*, *Nfe2l2*, *Nqo1*, and *Sqstm1* were observed. Compared
469 with the control, no changes in gene expression patterns were detected in the NAC group. C-D, In

L-02 cells, expression of *MYD88*, *TNF*, and *IL1B* were significantly dampened in NAC + PCB52 group, relative to the PCB52 group. Compared with the control, no changes in gene expression patterns were detected in the NAC group. *$p < 0.05$, **$p < 0.01$, compared with the control; #$p < 0.05$, ##$p < 0.01$, compared with the PCB52 group.

Figure 4. Western blot analysis for the expression of TLR4, MyD88, Traf6, NF-κB p65, Keap1, Nrf2, and HO-1 proteins. Increased expression of TLR4, MyD88, Traf6, and NF-κB p65 by PCB52 were significantly repressed by pretreatment with NAC in both Brl-3A (A-E) and L-02 cells (I-M), while no changes in the expression of Keap1, Nrf2, and HO-1 were observed (A, F-H, I, and N-P). Compared with the control, no changes in the expression of these proteins were detected in the NAC group. *$p < 0.05$, **$p < 0.01$, compared with the control; #$p < 0.05$, ##$p < 0.01$, compared with the PCB52 group.

Figure 5 Schematic diagrams of PCB52-induced hepatotoxicity *in vitro* and the alleviated effects of NAC.

Supplementary Figure 1. Cell viability examined by CCK-8 assay. PCB52 dose-dependently decreased cell viabilities in both Brl-3A and L-02 cells, especially at 40 and 80 μM. *$p< 0.05$, **$p< 0.01$, relative to the control.

Supplementary Figure 2. Cell viability in Brl-3A cells. No changes of cell viability were observed

491 in NAC alone treatment groups compared with the control. Cell viability was significantly reduced
492 by PCB52. The pretreatment of NAC (3 and 5 mM) significantly alleviated PCB52-induced
493 cytotoxicity. **$p < 0.01$, compared with the control; #$p < 0.05$, compared with the PCB52 group.

Figure 1

Detection of cell viabilities by CCK-8 assay

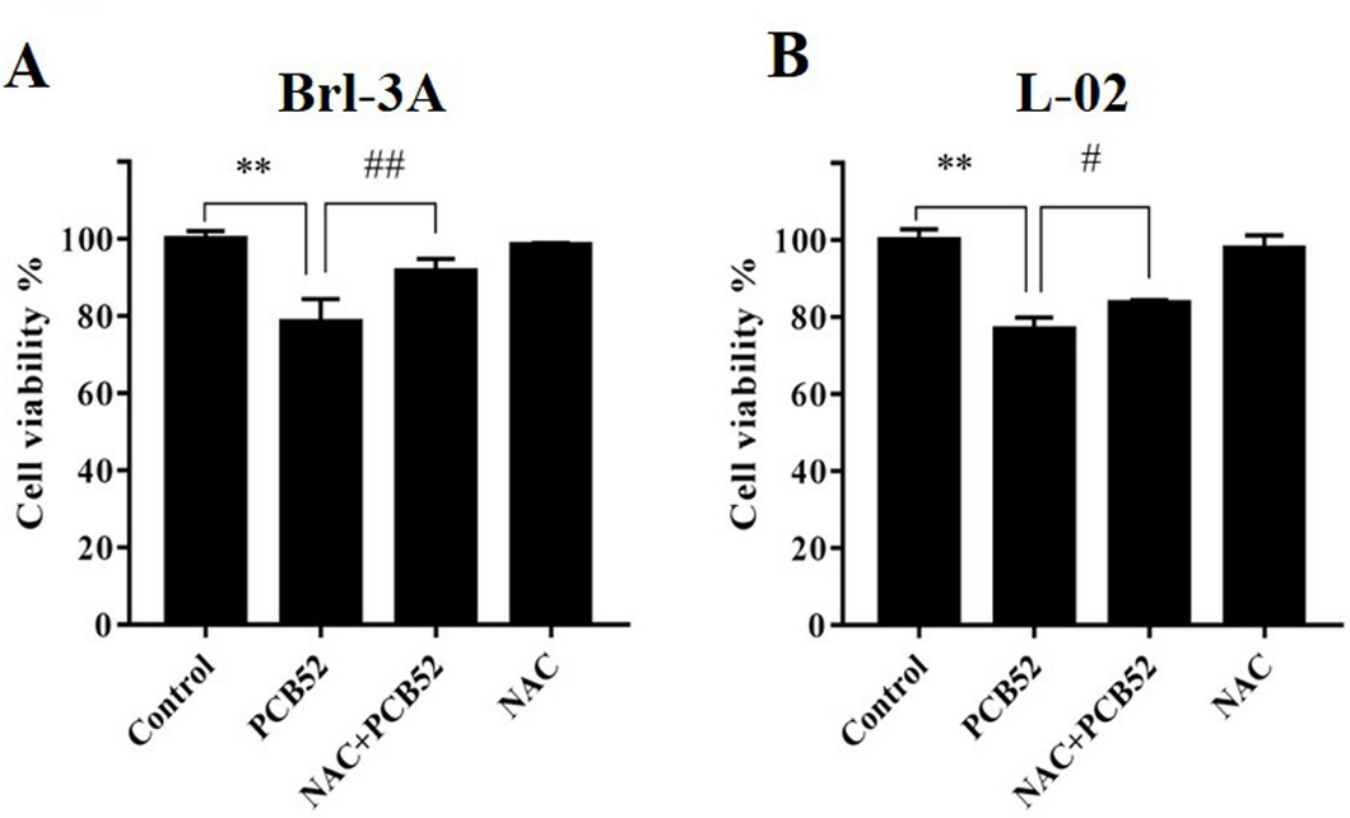

Figure 2

Examination of intracellular ROS levels and MDA contents

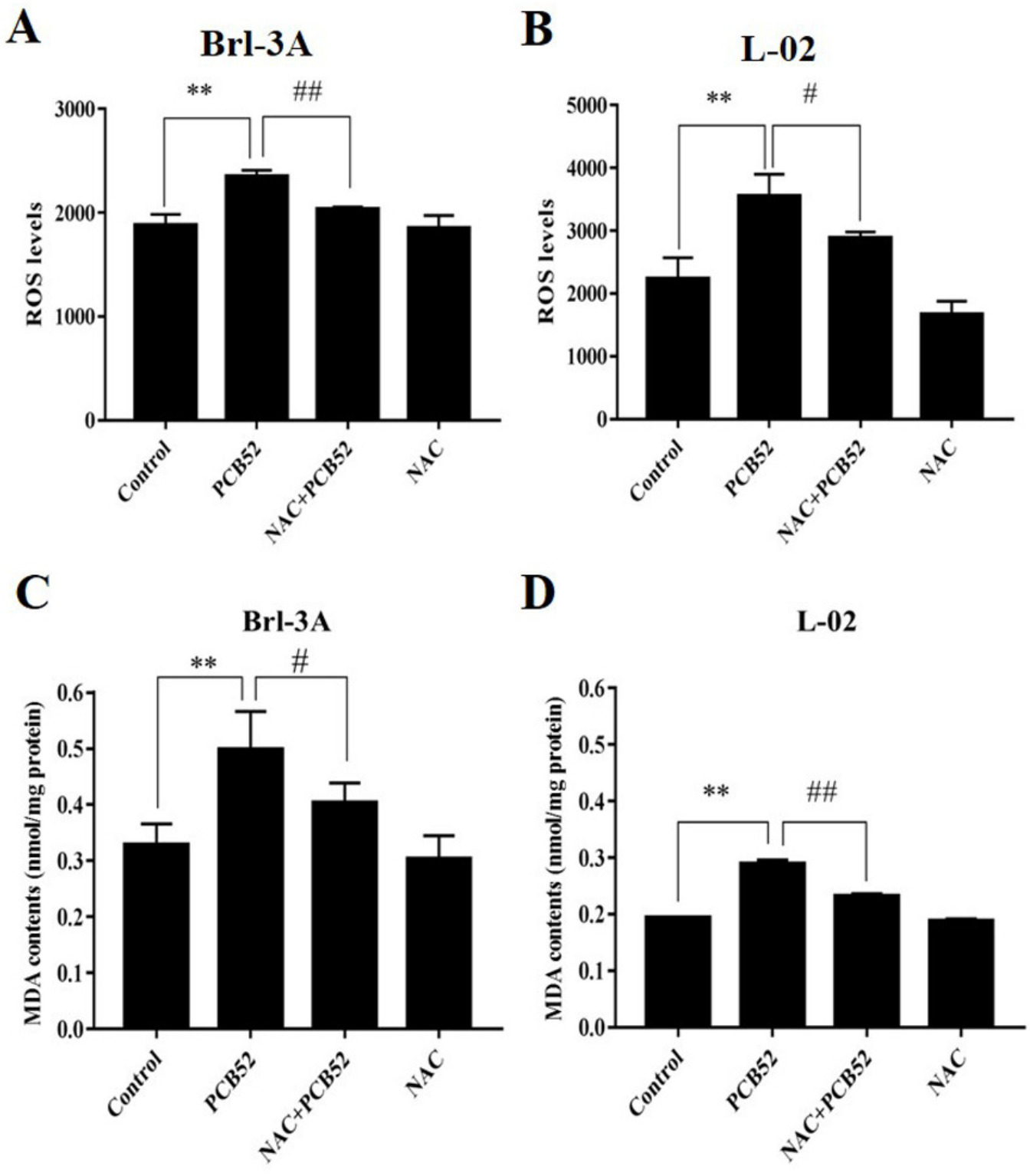
A
Brl-3A
**
##
ROS levels
3000
2000
1000
0
Control
PCB52
NAC+PCB52
NAC
B
L-02
**
#
ROS levels
5000
4000
3000
2000
1000
0
Control
PCB52
NAC+PCB52
NAC
C
Brl-3A
**
#
MDA contents (nmol/mg protein)
0.6
0.5
0.4
0.3
0.2
0.1
0.0
Control
PCB52
NAC+PCB52
NAC
D
L-02
**
##
MDA contents (nmol/mg protein)
0.6
0.5
0.4
0.3
0.2
0.1
0.0
Control
PCB52
NAC+PCB52
NAC

Figure 3

RT-qPCR analysis for assessment of *Traf6*, *MyD88*, *Tnf*, *IL1B*, *Keap1*, *Nfe2l2*, *Hmox1*, *Nqo1*, and *Sqstm1* gene expression

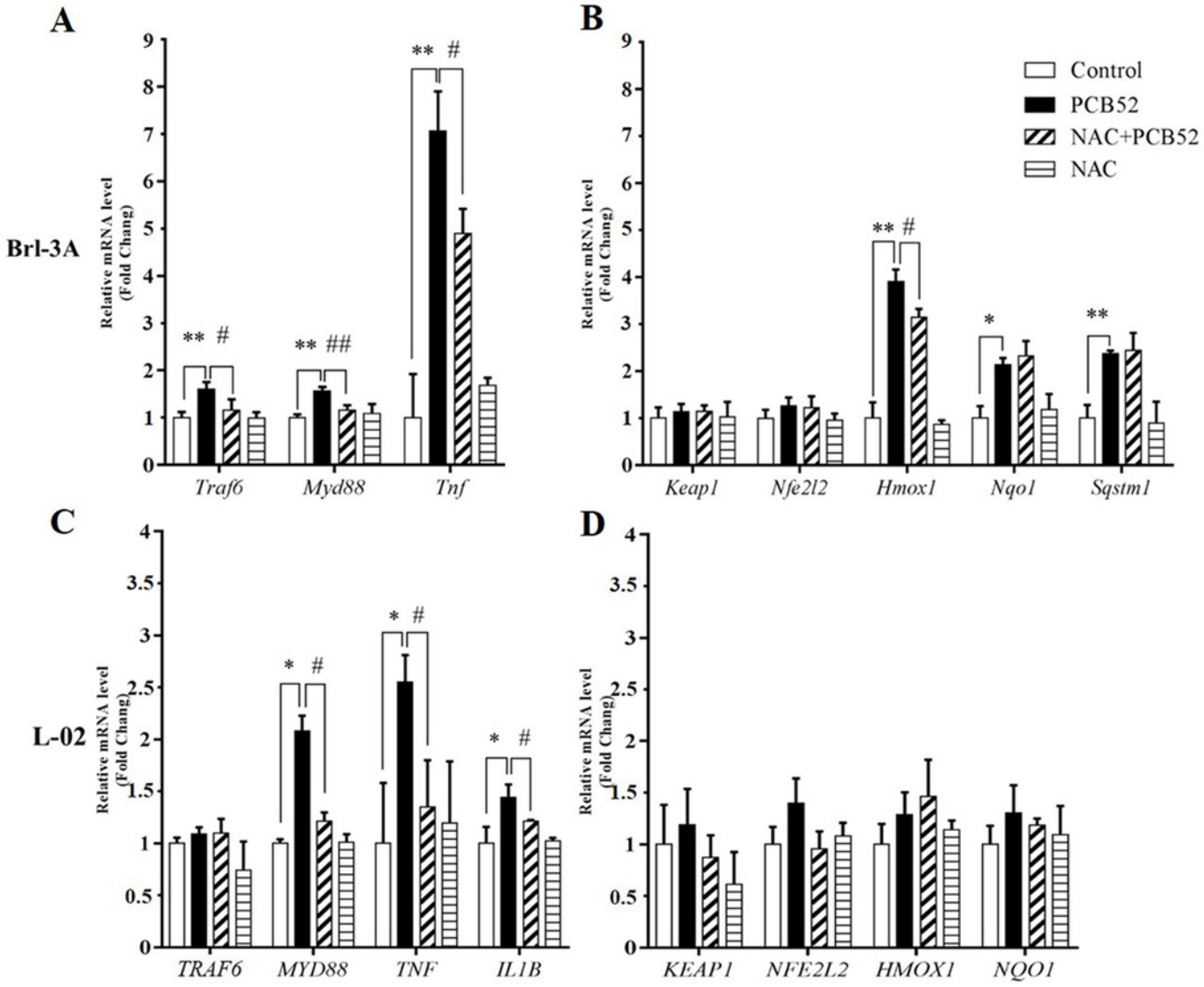

Figure 4

Western blot analysis for the expression of TLR4, MyD88, Traf6, NF-κB p65, Keap1, Nrf2, and HO-1 proteins

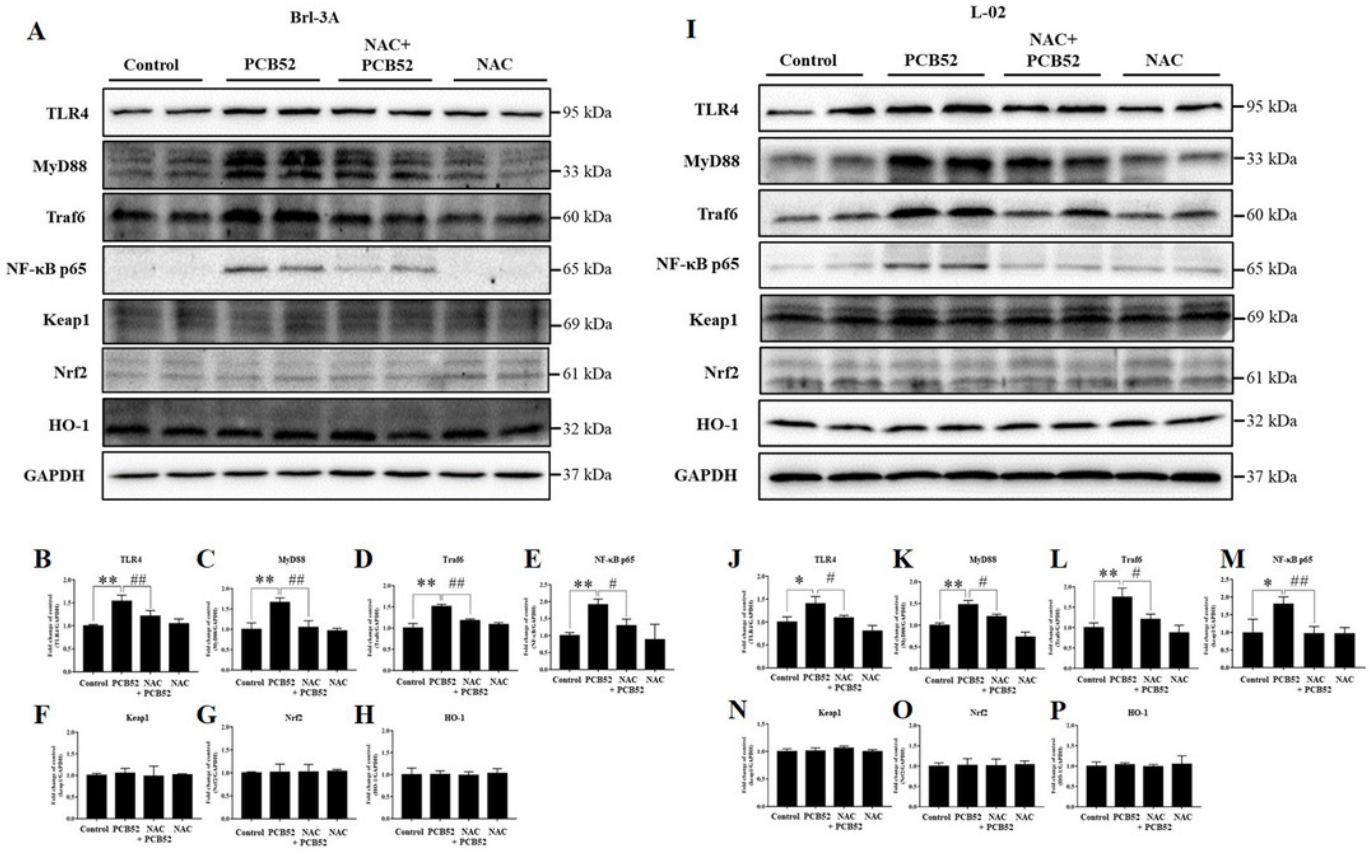

Figure 5
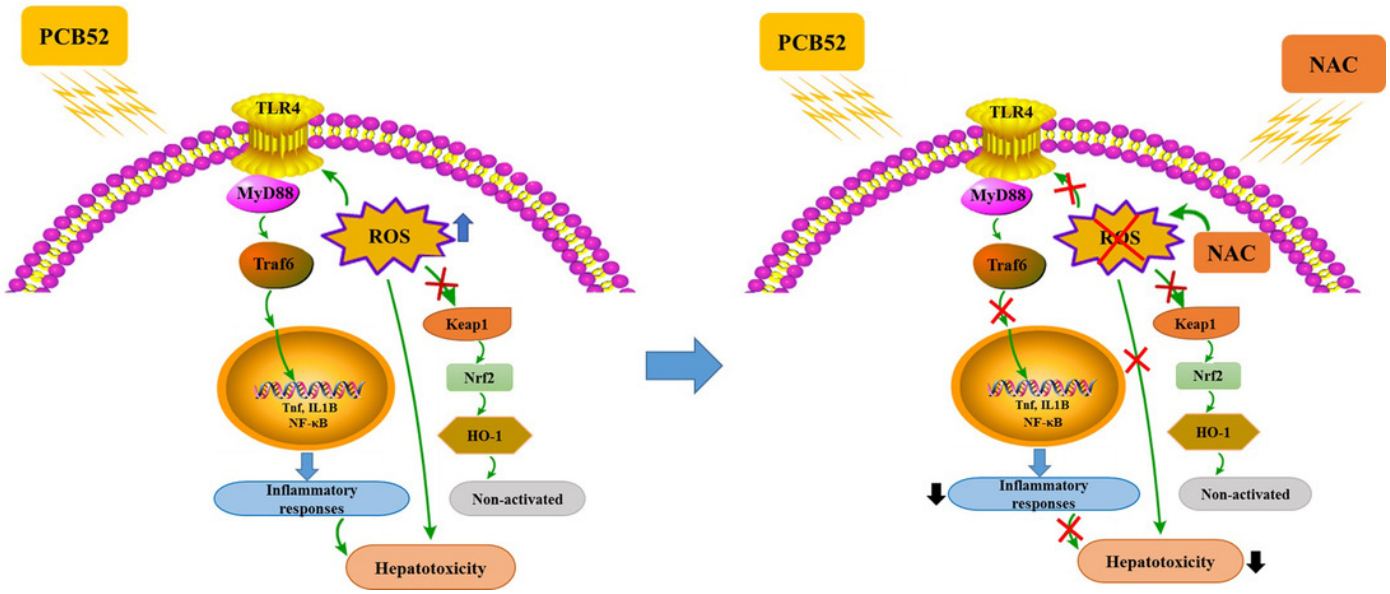
Schematic diagrams of PCB52-induced hepatotoxicity *in vitro* and the alleviated effects of NAC